SMC-TR-99-01

AEROSPACE REPORT NO.
TR-99(8570)-1

Cusp Energetic Ions: A Bow Shock Source

20 December 1998

Prepared by

S. -W. CHANG,[1] J. D. SCUDDER,[1] S. A. FUSELIER,[2]
J. F. FENNELL,[3] K. J. TRATTNER,[2] J. S. PICKETT,[1]
H. E. SPENCE,[4] J. D. MENIETTI,[1] W. K. PETERSON,[2]
R. P. LEPPING,[5] and R. FRIEDEL[6]

[1]University of Iowa
Iowa City, IA

[2]Lockheed Martin Advanced Technology Center
Palo Alto, CA

[3]The Aerospace Corporation
Los Angeles, CA

[4]Boston University
Boston, MA

[5]NASA Goddard Space Flight Center
Greenbelt, MD

[6]Los Alamos National Laboratory
Los Alamos, NM

Prepared for

SPACE AND MISSILE SYSTEMS CENTER
AIR FORCE MATERIEL COMMAND
2430 E. El Segundo Boulevard
Los Angeles Air Force Base, CA 90245

Engineering and Technology Group

THE AEROSPACE
CORPORATION
El Segundo, California

This report was submitted by The Aerospace Corporation, El Segundo, CA 90245-4691, under Contract No. F04701-93-C-0094 with the Space and Missile Systems Center, 2430 E. El Segundo Blvd., Los Angeles Air Force Base, CA 90245. It was reviewed and approved for The Aerospace Corporation by A. B. Christensen Principal Director, Space and Environment Technology Center. Col C. Whited was the project officer for the Mission-Oriented Investigation and Experimentation (MOIE) program.

This report has been reviewed by the Public Affairs Office (PAS) and is releasable to the National Technical Information Service (NTIS). At NTIS, it will be available to the general public, including foreign nationals.

This technical report has been reviewed and is approved for publication. Publication of this report does not constitute Air Force approval of the report's findings or conclusions. It is published only for the exchange and stimulation of ideas.

Peter Bissegger
SMC/AXES

REPORT DOCUMENTATION PAGE

Form Approved
OMB No. 0704-0188

1. AGENCY USE ONLY (*Leave blank*)

2. REPORT DATE
20 December 1998

3. REPORT TYPE AND DATES COVERED

4. TITLE AND SUBTITLE
Cusp Energetic Ions: A Bow Shock Source

5. FUNDING NUMBERS
F04701-93-C-0094

6. AUTHOR(S)
S. -W. Chang, J. D. Scudder, S. A. Fuselier, J. F. Fennell, K. J. Trattner, J. S. Pickett, H. E. Spence, J. D. Menietti, W. K. Peterson, R. P. Lepping, and R. Friedel

7. PERFORMING ORGANIZATION NAME(S) AND ADDRESS(ES)
The Aerospace Corporation
Technology Operations
El Segundo, CA 90245-4691

8. PERFORMING ORGANIZATION REPORT NUMBER
TR-99(8570)-1

9. SPONSORING/MONITORING AGENCY NAME(S) AND ADDRESS(ES)
Space and Missile Systems Center
Air Force Materiel Command
2430 E. El Segundo Boulevard
Los Angeles Air Force Base, CA 90245

10. SPONSORING/MONITORING AGENCY REPORT NUMBER
SMC-TR-99-01

11. SUPPLEMENTARY NOTES

12a. DISTRIBUTION/AVAILABILITY STATEMENT
Approved for public release; distribution unlimited

12b. DISTRIBUTION CODE

13. ABSTRACT (*Maximum 200 words*)
Recent interpretations of cusp energetic ions observed by the POLAR spacecraft have suggested a new energization process in the cusp [*Chen et al.*, 1997, 1998]. Simultaneous enhancement of H^+, He^{+2}, and $O^{>+2}$ fluxes indicates that they are of solar wind origin. In the present study, we examine H^+ and He^{+2} energy spectra from 20 eV to several 100 keV measured by the Hydra, Toroidal Imaging Mass-Angle Spectrograph (TIMAS), and Charge and Mass Magnetospheric Ion Composition Experiment (CAMMICE) on POLAR. The combined spectrum for each species is shown to be continuous with a thermal distribution below 10 keV and an energetic component above 20 keV/e. Energetic ions with comparable fluxes and a similar spectral shape are commonly observed downstream from the Earth's quasi-parallel bow shock. In addition to the similarity in the ion spectra, electric and magnetic field noise and turbulence detected in the cusp by the Plasma Wave Instrument (PWI) and Magnetic Field Experiment (MFE) onboard POLAR are similar to the previously reported observations at the bow shock. The waves appear to be coincidental to the cusp energetic ions rather than causal. We suggest that these ions are not accelerated locally in the cusp. Rather, they are accelerated at the quasi-parallel bow shock and enter the cusp along open magnetic field lines connecting both regions.

14. SUBJECT TERMS
Cusp, Energetic particles, POLAR satellite

15. NUMBER OF PAGES
5

16. PRICE CODE

17. SECURITY CLASSIFICATION OF REPORT	18. SECURITY CLASSIFICATION OF THIS PAGE	19. SECURITY CLASSIFICATION OF ABSTRACT	20. LIMITATION OF ABSTRACT
UNCLASSIFIED	UNCLASSIFIED	UNCLASSIFIED	

NSN 7540-01-280-5500

Standard Form 298 (Rev. 2-89)
Prescribed by ANSI Std. Z39-18
298-102

Acknowledgments

This work was supported at Iowa University (Hydra, PWI), Lockheed Martin (TIMIS), Aerospace (CAMMICE), and MPAE (Hydra) by grants from NASA (NAG 5 2231, NAS5-30371, NAS5-30302, NAS5-30368), Boston University (GC 131165 NGD), and DARA (50 OC 8911 0), respectively. The work at Aerospace was supported in part by Air Force Contract No. F04701-93-C-0094 and Boston University contract GC 131165 NGD. WSC would like to thank W. J. Burke for useful discussions. We thank C. T. Russell for MFE magnetic field data. We are grateful to R. D. Holdaway, J. Faden, P. Puhl-Quinn, and J. C. Dorelli for Hydra software activities. The present results of the Hydra investigation were made possible by the decade-long hardware efforts of groups led at NASA GSFC by K. Ogilvie, at UNH by R. Torbert, at MPAE by A. Korth, and UCSD by W. Fillius.

Contents

Figures

Introduction

Plasmas in the cusp with energies less than several keV/e, except for the low-energy (less than ~100 eV) ionospheric component, have been long understood to be directly from the solar wind. The energetic particle data from the POLAR spacecraft recently called into question the origin of high-energy plasmas in the cusp. These cusp energetic particles (CEPs) first documented in the CAMMICE and CEPPAD data have energies above the typical solar wind energies up to hundreds of keV/e [*Chen et al.*, 1997, 1998]. Ion composition measurements show that they are of solar wind origin. Because energetic particles were not observed in the solar wind during the CEP events, the authors suggest that CEPs are accelerated locally in the cusp. Since ions gain up to about twice the Alfvén speed (correspond to ~1 keV) across the magnetopause current layer [e.g., *Cowley*, 1982], this acceleration cannot account for the observed high energies of solar wind ions. However, an important source of energetic ions that was ignored in the previous study is the Earth's bow shock.

Energetic ions are ubiquitous upstream and downstream from the $Q_{||}$ bow shock. Numerous observations [e.g., *Ipavich et al.*, 1981; *Möbius et al.*, 1987; *Gosling et al.*, 1989; *Ellison et al.*, 1990; *Fuselier et al.*, 1995, and references therein], theoretical work [e.g., *Lee*, 1982], and simulations [e.g., *Ellison et al.*, 1990] have shown that ions at the $Q_{||}$ bow shock contain a Maxwellian core distribution as well as an energetic tail distribution with energies up to several hundred keV and above. Solar wind ions are energized to these energies via the first-order Fermi acceleration process. All the ion species have a similar spectral shape with the same e folding at ~20 keV/e. The ion energy spectrum mainly depends on the solar wind density and velocity [*Trattner et al.*, 1994]. Energetic ions downstream from the $Q_{||}$ bow shock are nearly isotropic and flow away from the shock. In this paper, we present POLAR plasma and field data acquired in the cusp during CEP events and relate these to observations at the bow shock. We suggest that the observed cusp energetic ions simply come from the solar wind after acceleration at the shock.

Observations

On June 20, 1996, Hydra [*Scudder et al.*, 1995] and CAMMICE detected intense ion fluxes from 6 to 7 UT while POLAR was traveling poleward through the northern cusp. Cold, magnetosheath-like electrons were also measured by Hydra during this interval. The average energies for the electrons and ions are ~30 and ~350 eV, respectively. Figure 1 shows the spin-averaged ion distribution function from 0602 to 0658 UT. Hydra ions (assuming H^+) with energies from 17 eV to 19 keV (corrected by the spacecraft potential) from detectors 9 and 10 of the DuoDeca Electron Ion Spectrometer (DDEIS) are indicated by triangles. CAMMICE data are the total ion measurements assuming H^+ response in the Double Coincidence Rate (DCR) channel of the Magnetospheric Ion Composition Sensor (MICS) from 1 to 270 keV indicated by squares. A similar detector was flown on the CRRES satellite [*Wilken et al.*, 1992]. The two Hydra detectors were chosen to match the viewing direction of the MICS detector. Both instruments are well inter-calibrated for this event as illustrated by the match between triangles and squares over the energy overlap (1-20 keV). Small differences are attributed to different efficiency for different ion species in the two instruments. The whole spectrum is continuous with a Maxwellian (< 10 keV) distribution and a non-thermal (> 20 KeV) component which is fit by a power law with an index of 4.73. The MICS fluxes above ~150 keV were low and close to the cosmic ray background. Energetic and high charge-state ion (He^{+2} and $O^{>+2}$) fluxes detected by CAMMICE like the H^+ flux were also simultaneously enhanced in the cusp. It suggests that the cusp energetic ions originated in the solar wind.

Interplanetary magnetic field (IMF) data acquired with the WIND Magnetic Field Investigation (MFI) [*Lepping et al.*, 1995] during this CEP event are pre-

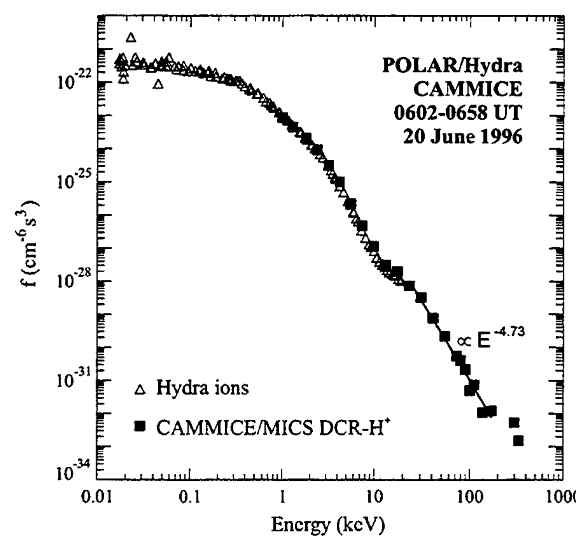

Figure 1. Ion energy spectrum measured by Hydra and CAMMICE on June 20, 1996. See text for details.

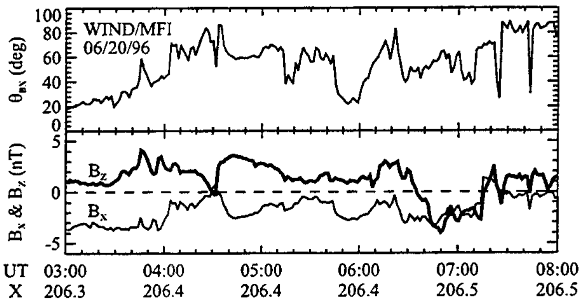

Figure 2. IMF cone angles and GSM components measured by WIND/MFI on June 20, 1996.

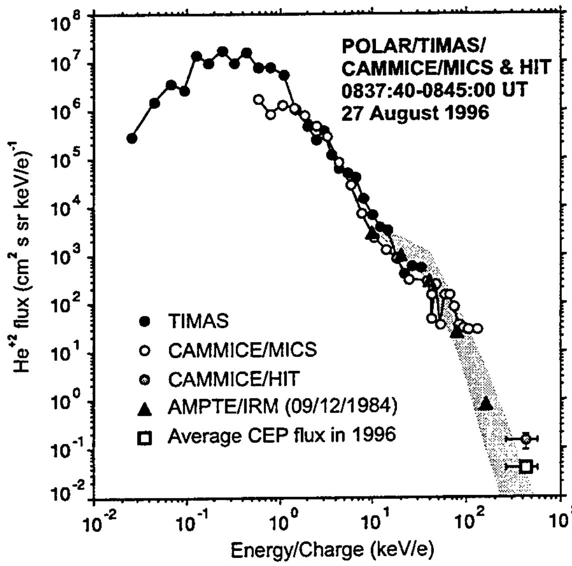

Figure 3. He^{+2} spectrum measured by TIMAS and CAMMICE on August 27, 1996. See text for details.

sented in Figure 2. The averaged solar wind speed obtained from the WIND Solar Wind Experiment [*Ogilvie et al.*, 1995] was $\sim$450 km/s. Estimated time delay for solar wind propagating from WIND to the subsolar bow shock is $\sim$45 mins. Since WIND was located within 7° of the Sun-Earth line, IMF B_x (B_z) was likely negative (positive) at the magnetopause during this event. The angle between the IMF and the Sun-Earth line, i.e., the cone angle (θ_{BX}), was mostly less than 65° from 0515 to 0615 UT. This IMF geometry suggests that the $Q_{\|}$ bow shock was located during this CEP event in the sunlit southern hemisphere, near the nose.

He^{+2} spectrum from TIMAS [*Shelley et al.*, 1995] and CAMMICE for another CEP event on August 27, 1996 [*Chen et al.*, 1997] is shown in Figure 3. The TIMAS data presented here have not been corrected for a count rate dependent spill over from the coexisting H^+ population. This contamination accounts for the discrepancy between TIMAS and CAMMICE fluxes below $\sim$1 keV/e. Otherwise, TIMAS and CAMMICE data agree well. Similar to the H^+ spectrum in Figure 1, the He^{+2} spectrum has a non-thermal component above $\sim$20 keV/e. The IMF conditions here are similar to the June 20 event, i.e., $B_x < 0$, $B_z > 0$, and $\theta_{BX} < 65°$. To compare the observations in the cusp with those at a possible bow shock source location, AMPTE/IRM observations downstream from a "typical" $Q_{\|}$ bow shock taken from Figure 2a of *Ellison et al.* [1990] are plotted in Figure 3. The agreement between the energetic He^{+2} spectra at two locations is quite remarkable, suggesting that the cusp spectrum is directly extracted from the parent bow shock source region.

To further compare the cusp and bow shock spectra, a range of the He^{+2} fluxes downstream from the $Q_{\|}$ bow shock is shown in Figure 3 as the shaded region. The AMPTE/IRM SULEICA data were selected in the 1986 database for similar solar wind density and bulk speed and IMF orientation as observed on August 27, 1996. Spectra are extended beyond 160 keV/e according to a power-law relation from the data detected at the last two energy channels for easy comparison with the "MeV" ion flux observed by the CAMMICE/HIT detector. The HIT flux is calculated from Figure 1 of *Chen et al.* [1997] assuming that Helium ion charge state was +2. Because the energy band pass of the HIT detector is very wide, 0.52-1.15 MeV, the observed flux could be the response near the lower limit of the pass band at 260 keV/e which corresponds to 0.52 MeV total energy. By taking into account this uncertainty, the HIT flux is consistent with the bow shock spectrum. The averaged HIT flux of the 1996 CEP events from Figure 7 of *Chen et al.* [1998] is even lower and well described by the average AMPTE/IRM bow shock spectrum.

Low-frequency electric and magnetic noise and turbulence are commonly detected by PWI [*Gurnett et al.*, 1995] and MFE [*Russell et al.*, 1995] onboard POLAR during the CEP events. Preliminary study of PWI observations indicates that intense low-frequency turbulence of large temporal/spatial scale is rare when CEPs are absent. As shown in Figure 4, wave energy density from PWI integrated from 4.9 Hz to 10.56 (336.6) kHz for the 1-D magnetic (electric) component is roughly 5 orders of magnitude less than the plasma energy density for the June 20 event. Because this component is

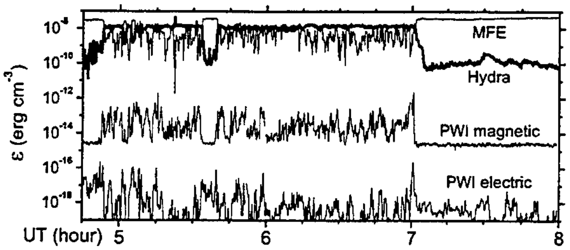

Figure 4. Comparison of wave (PWI and MFE) and particle (Hydra) energy density on June 20, 1996.

greater than or comparable to the other two components, the total wave energy density would probably be well below the plasma energy density. Assuming no spatial variation and DC component in the MFE magnetic field data, the maximum ULF wave magnetic energy density is only ~10% of the plasma energy density. This excludes the energy of the energetic ions which would increase this discrepancy. Low-frequency waves accompanying energetic ions are also frequently observed at the $Q_{||}$ bow shock [e.g., *Paschmann et al.*, 1979]. Wave energy density there is comparable to the value in the cusp [*Möbius et al.*, 1987].

Discussions and Conclusions

Most CEP events occurred in 1996 under IMF $B_x < 0$, $B_z > 0$ conditions [*Finkemeyer et al.*, 1998]. We have examined more than 6 months of POLAR and WIND data for the northern cusp and note that besides the above condition, the IMF cone angle (θ_{BX}) is relatively small during CEP events. In addition, CEPs are rare when $B_z < 0$ and θ_{BX} is relatively large. The two CEP events presented above are typical examples. Both the cusp H^+ and He^{+2} spectra are similar to those downstream from the $Q_{||}$ bow shock. The observed cusp energetic ions can be simply explained by a model of transporting bow shock accelerated ions across the magnetopause into the cusp along interconnected field lines.

The concept is illustrated in Figure 5. IMF points north and away from the Sun. As the IMF field line A and the lobe field line B approach each other, they reconnect at the point X at the high-latitude magnetopause according to the anti-parallel merging hypothesis [*Crooker*, 1979]. It results in a new open magnetic field line C convecting sunward at the magnetopause and a new IMF field line D convecting tailward in the magnetosheath. The field line C is connected to the poleward edge of the northern cusp and sweeps through

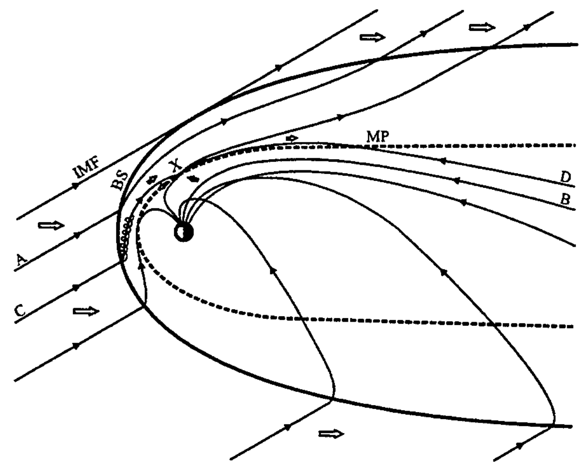

Figure 5. Schematic diagram of the geospace for IMF $B_x < 0$ and $B_z > 0$. Heavy lines are the bow shock (solid) and the magnetopause (dashed). B field lines are plotted in 3-D perspective to show their evolution. Open arrows indicate the plasma flow direction.

the cusp as it convects sunward. It is also connected to the southern portion of the bow shock near the subsolar region where the shock surface is $Q_{||}$ downstream from the ion foreshock for a small θ_{BX}. Downstream from the $Q_{||}$ shock, energetic ions are nearly isotropic flowing away from the shock [e.g., Figure 5b of *Ellison et al.*, 1990]. These ions simply follow the newly opened field lines and directly enter the cusp. As the cusp field line convects duskward (or dawnward) at the magnetopause and tailward at the bow shock away from the nose, it evolves into a lobe field line. Because the connection time for ions and waves is much reduced downtail of the shock [*Ellison et al.*, 1990], fluxes of energetic ions there diminish and would not enter the polar cap. Eventually the ion bulk speed becomes super-sonic and almost all the thermal ions cannot move against the flow across the magnetopause. Observable precipitation into the polar cap mainly comes from electrons as the polar rain.

When IMF $B_z < 0$ with a large θ_{BX}, dayside merging site shifts toward lower latitude of the magnetopause equatorward of the cusp and the subsolar region of the bow shock is quasi-perpendicular where Fermi acceleration does not occur. Newly merged cusp field lines convect tailward both at the magnetopause and at the bow shock in the same hemisphere. In this case, the $Q_{||}$ shock is located near the flank. For the same reason discussed above, ions there are energized to lower energies than for the $Q_{\|}$ shock with a smaller θ_{BX} case and they flow downtail in the magnetosheath further away from the cusp. This is consistent with the observation of low energetic ion fluxes during such IMF conditions.

Another important factor for determining the cusp location is the dipole tilt angle. For a tilt angle away from the Sun as is the case during the winter season in the northern hemisphere, the southern cusp is closer to the subsolar point than the northern cusp. Dayside merging takes place in the southern hemisphere first and may not take place in the northern hemisphere for a northward IMF condition. Energetic ions downstream from the $Q_{\|}$ bow shock would not have access to the northern cusp. This seasonal effect has been found in the 1996 CEP statistics [*Chen et al.*, 1998]. A similar effect was also found in the low-altitude cusp statistics from the DMSP spacecraft [*Newell and Meng*, 1988]. In this case however, few thermal ions precipitate into the cusp because the ratio of the magnetosheath ion bulk flow speed and thermal speed increases away from the subsolar point.

The low-frequency electric/magnetic noise and turbulence observed by POLAR in the cusp during CEP events have an energy density less than 10% of the plasma energy density. This would require a very efficient way of converting the wave energy into the plasma energy to produce the high energy tail. Such a mechanism has not been proposed [*Chen et al.*, 1998]. We note that one cannot simply argue whether the wave amplitude implys the plasma energization or not. Wave-particle interaction, such as gyro-resonance and Landau process, can produce ion heating. However, as shown above, the observed cusp ion spectra are similar to those at the bow shock source. Waves of the same frequency and comparable power are also observed at the $Q_{\|}$ bow shock. Besides, a statistical study using more than two years of Hawkeye 1 data shows that ULF-ELF magnetic noise is nearly always present in the cusp [*Gurnett and Frank*, 1978], whereas CEPs occur under preferred IMF orientation and season. Thus the waves are most probably coincidental to CEPs rather than causal.

In summary, IMF orientation controls the bow shock geometry, the dayside merging site and the magnetic topology. Energetic ion fluxes downstream from the $Q_{\|}$ bow shock are comparable to those observed in the cusp. The waves are probably incidental. The cusp and the $Q_{\|}$ bow shock are magnetically interconnected during CEP events. Therefore, bow shock accelerated ions can simply follow the open field lines and enter the cusp.

References

Chen, J. et al., A new, temporarily confined population in the polar cap during the August 27, 1996 geomagnetic field distortion period, *Geophys. Res. Lett., 24,* 1447, 1997.

Chen, J. et al., Cusp energetic particle events: Implications for a major acceleration region of the magnetosphere, *J. Geophys. Res., 103,* 69, 1998.

Cowley, S. W. H., The causes of convection in the Earth's magnetosphere: A review of developments during the IMS, *Rev. Geophys., 20,* 531, 1982.

Crooker, N. R., Dayside merging and cusp geometry, *J. Geophys. Res., 84,* 951, 1979.

Finkemeyer, B. et al., Possible association of cusp energetic particle events with interplanetary conditions (abstract), *Eos Trans. AGU, 79*(17), Spring Meet. Suppl., S298, 1998.

Fuselier, S. A. et al., Suprathermal He^{2+} in the Earth's foreshock region, *J. Geophys. Res., 100,* 17,107, 1995.

Ellison, D. C. et al., Particle injection and acceleration at Earth's bow shock: Comparison of upstream and downstream events, *Astrophys. J., 352,* 376, 1990.

Gosling, J. T. et al., On the source of diffuse, suprathermal ions observed in the vicinity of the Earth's bow shock, *J. Geophys. Res., 94,* 3555, 1989.

Gurnett, D. A., and L. A. Frank, Plasma waves in the polar cusp: Observations from Hawkeye 1, *J. Geophys. Res., 83,* 1447, 1978.

Gurnett, D. A. et al., The POLAR plasms wave instrument, *Space Sci. Rev., 71,* 597, 1995.

Ipavich, F. M. et al., Temporal development of composition, spectra, and anisotropies during upstream particle events, *J. Geophys. Res., 86,* 11,153, 1981.

Lee, M. A., Coupled hydromagnetic wave excitation and ion acceleration upstream of the Earth's bow shock, *J. Geophys. Res., 87,* 5063, 1982.

Lepping, R. P. et al., The WIND magnetic field investigation, *Space Sci. Rev., 71,* 207, 1995.

Möbius, E. et al., The distribution function of diffuse ions and the magnetic field power spectrum upstream of Earth's bow shock, *Geophys. Res. Lett., 14,* 681, 1987.

Newell, P. T., and C.-I. Meng, Hemispherical asymmetry in cusp precipitation near solstices, *J. Geophys. Res., 93,* 2643, 1988.

Ogilvie, K. W. et al., SWE, a comprehensive plasma instrument for the WIND spacecraft, *Space Sci. Rev., 71,* 55, 1995.

Paschmann, G. et al., Association of low-frequency waves with suprathermal ions in the upstream solar wind, *Geophys. Res. Lett., 6,* 209, 1979.

Russell, C. T. et al., The GGS/POLAR magnetic field investigation, *Space Sci. Rev., 71,* 563, 1995.

Scudder, J. D. et al., Hydra-A 3-dimensional electron and ion hot plasma instrument for the POLAR spacecraft of the GGS mission, *Space Sci. Rev., 71,* 459, 1995.

Shelley, E. G. et al., The toroidal imaging mass-angle spectrograph (TIMAS) for the POLAR mission, *Space Sci. Rev., 71,* 497, 1995.

Trattner, K. J. et al., Statistical analysis of diffuse ion events upstream of the Earth's bow shock, *J. Geophys. Res., 99,* 13,389, 1994.

Wilken, B. et al., Magnetospheric ion composition spectrometer onboard the CRRES Spacecraft, *Journal Spacecraft and Rockets, 29,* 585, 1992.

TECHNOLOGY OPERATIONS

The Aerospace Corporation functions as an "architect-engineer" for national security programs, specializing in advanced military space systems. The Corporation's Technology Operations supports the effective and timely development and operation of national security systems through scientific research and the application of advanced technology. Vital to the success of the Corporation is the technical staff's wide-ranging expertise and its ability to stay abreast of new technological developments and program support issues associated with rapidly evolving space systems. Contributing capabilities are provided by these individual Technology Centers:

Electronics Technology Center: Microelectronics, VLSI reliability, failure analysis, solid-state device physics, compound semiconductors, radiation effects, infrared and CCD detector devices, Micro-Electro-Mechanical Systems (MEMS), and data storage and display technologies; lasers and electro-optics, solid state laser design, micro-optics, optical communications, and fiber optic sensors; atomic frequency standards, applied laser spectroscopy, laser chemistry, atmospheric propagation and beam control, LIDAR/LADAR remote sensing; solar cell and array testing and evaluation, battery electrochemistry, battery testing and evaluation.

Mechanics and Materials Technology Center: Evaluation and characterization of new materials: metals, alloys, ceramics, polymers and composites; development and analysis of advanced materials processing and deposition techniques; nondestructive evaluation, component failure analysis and reliability; fracture mechanics and stress corrosion; analysis and evaluation of materials at cryogenic and elevated temperatures; launch vehicle fluid mechanics, heat transfer and flight dynamics; aerothermodynamics; chemical and electric propulsion; environmental chemistry; combustion processes; spacecraft structural mechanics, space environment effects on materials, hardening and vulnerability assessment; contamination, thermal and structural control; lubrication and surface phenomena; microengineering technology and microinstrument development.

Space and Environment Technology Center: Magnetospheric, auroral and cosmic ray physics, wave-particle interactions, magnetospheric plasma waves; atmospheric and ionospheric physics, density and composition of the upper atmosphere, remote sensing, hyperspectral imagery; solar physics, infrared astronomy, infrared signature analysis; effects of solar activity, magnetic storms and nuclear explosions on the earth's atmosphere, ionosphere and magnetosphere; effects of electromagnetic and particulate radiations on space systems; component testing, space instrumentation; environmental monitoring, trace detection; atmospheric chemical reactions, atmospheric optics, light scattering, state-specific chemical reactions and radiative signatures of missile plumes, and sensor out-of-field-of-view rejection.